Electronic Supplementary Material (ESI) for Physical Chemistry Chemical Physics.

Supporting Information for

Coarse-Grained Molecular Dynamics Study on the Self-assembly of Gemini Surfactants: Effect of Spacer Length

Pan Wang[ab], Shuai Pei[ab], Muhan Wang[ab], YouguoYan[ab],XiaoliSun[*a],and Jun Zhang[*ab]

†College of Science, China University of Petroleum, 266580 Qingdao, Shandong, China

‡Key Laboratory of New Energy Physics & Materials Science in Universities of Shandong, China University of Petroleum, 266580 Qingdao, Shandong, China

***Corresponding Authors**

XiaoliSun and Jun Zhang

E-mail address: sunxiaoli@upc.edu.cn; zhangjun.upc@gmail.com

1. Force field development

Several parameters needed were not clearly specified in the Martini force field[1], such as the bond interaction parameter Q_0-Spacer and the angle interaction parameter C_2-Q_0-Spacer of 16-8-16, the bond interaction parameter Q_0-Q_0 and the angle interaction parameter C_2-Q_0-Q_0 of 16-4-16 and 16-2-16. These interactions were calculated by a weak harmonic potential U_{Bonded} (eq. 1), which had been extensively used in Coarse-grained force field development[1, 2].

$$U_{Bonded} = U_{stretch} + U_{bend} = \frac{1}{2} K_{stertch} (R - R_0)^2 + \frac{1}{2} K_{bend} (\cos(\theta) - \cos(\theta_0))^2 \quad (1)$$

where $U_{stretch}$ and U_{bend} represent the bond stretch and angle bend potentials, respectively. $K_{stertch}$ and K_{bend} are spring constants. R_0 and θ_0 are equilibrium constants. The interaction parameters were adjusted by comparing corresponding bonds and angles, which were obtained from atomistic simulations, respectively. Firstly, the preassembled spherical micelle (Fig. S1 (a)) consisting of 80 CTAC surfactants was constructed by Packmol[3] software and then solvated with SPC water[4] in the cubic box with dimension 5nm, and the GROMOS96 45a3 force filed was exploited which has been proved to accurately provide structural properties of CTAC/CTAB micelles solutions[5-7]. Secondly, AA MD was performed by the Gromacs[8] package. The Isothermal-Isobaric ensemble NPT was performed at 298 K and 1 atm for each system, with periodic boundary conditions along three directions. The temperature was controlled by the Berendsen thermostat[9], and the pressure coupling was set as the Berendsen barostat[9]. A fixed time step of 0.002 ps was used and a 10 ns simulation time was performed, the last 5 ns was used for the data analysis. Thirdly, the bond stretch and angle bend distributions of the center of mass (COM) of different molecular fragments (Coarse grained to beads, defined in Fig. 1) were generated and shown in Fig. S2 (black line). Fourthly, the Coarse-grained model

correspond to the AA MD system was established (Fig. S1 (b)), the simulation details was same as main text, and the total simulation time was 20 ns, the last 10 ns was used for the data analysis. Finally, the bond stretch and angle bend distribution of CG MD were generated. The CG Bonded interactions were adjusted successively until the bond stretch and angle bend distribution of CG is consistent with AA (Fig. S2). All the interaction parameters are shown in Table S1 and Table S2.

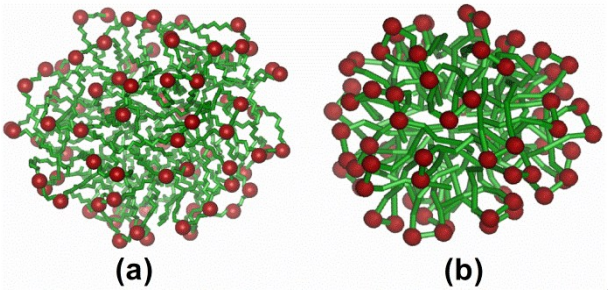

Figure S1. Representative snapshots of micelles for Gemini surfactant. (a) AA model and (b) CG model with the number of surfactants equal to 40. For clarity, water is not shown.

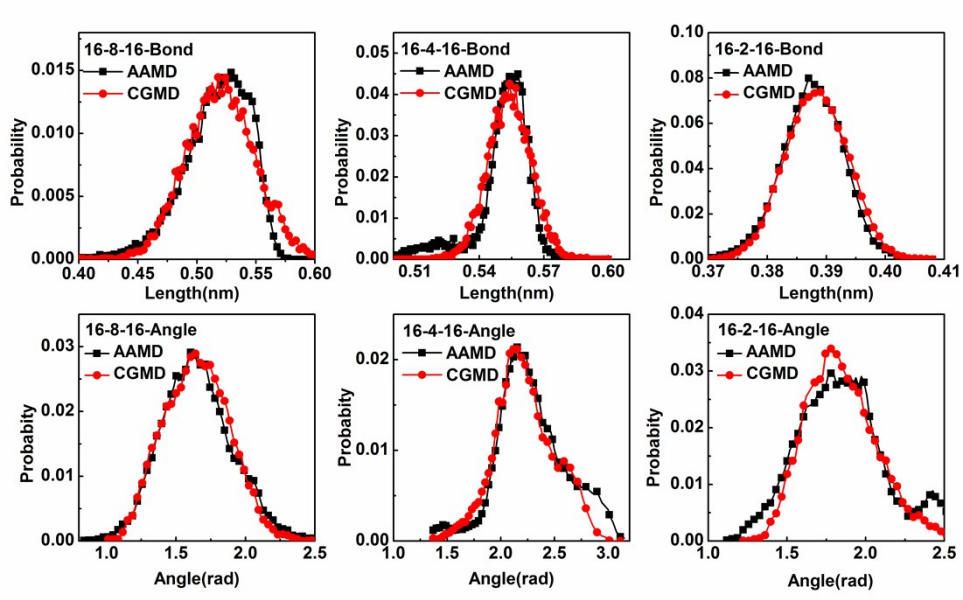

Figure S2 The length distribution and angle distribution for 16-8-16, 16-4-16 and 16-2-16, respectively. Compared between AAMD (black) and CGMD (Red).

Table S1 The final bonded parameters for 16-s-16 , CTAC, SDS and NaSal

	Bond parameters		Angle parameters	
16-8-16	Q_0-Spacer		C_2-Q0-Spacer	
	$K_{stertch}$ ($kJ \cdot mol^{-1} \cdot nm^{-2}$)	R_0 (Å)	K_{bend} $kJ\ mol^{-1}$	θ_0 (º)
	10000	5.3	80	92
16-4-16	Q_0-Spacer		C_2-Q0- Q0	
	$K_{stertch}$ ($kJ \cdot mol^{-1} \cdot nm^{-2}$)	R_0 (Å)	K_{bend} $kJ\ mol^{-1}$	θ_0 (º)
	100000	3.88	40	120
16-2-16	Q_0-Spacer		C_2-Q0- Q0	
	$K_{stertch}$ ($kJ \cdot mol^{-1} \cdot nm^{-2}$)	R_0 (Å)	$K_{stertch}$ $kJ\ mol^{-1}$	θ_0 (º)
	22000	5.55	80	125
NaSal	SC_4-SC_4		SC_4-SC_4-SC_4	
	$K_{stertch}$ ($kJ \cdot mol^{-1} \cdot nm^{-2}$)	R_0 (Å)	$K_{stertch}$ $kJ\ mol^{-1}$	θ_0 (º)
	constraint	2.7	0	0
CTAC, 16-s-16,SDS, NaSal	The others		The others	
	$K_{stertch}$ ($kJ \cdot mol^{-1} \cdot nm^{-2}$)	R_0 (Å)	$K_{stertch}$ $kJ\ mol^{-1}$	θ_0 (º)
	1250	4.7	45	180

Table S2 The final non-bonded parameters for 16-s-16 , CTAC, SDS and NaSal

Bead-1		Bead-2	Function	ε $kJ\ mol^{-1}$	σ (Å)
name	charge	name			
C_1	0.0	C_1	LJ12-6	3.5	4.7
C_1	0.0	C_2	LJ12-6	3.5	4.7
C_1	0.0	Q_0	LJ12-6	2.0	6.2
C_1	0.0	Q_a	LJ12-6	2.0	6.2
C_1	0.0	P_4	LJ12-6	2.0	4.7
C_1	0.0	BP_4	LJ12-6	2.0	4.7
C_2	0.0	C_2	LJ12-6	3.5	4.7

C_2	0.0	Q_0	LJ12-6	2.0	6.2
C_2	0.0	Q_a	LJ12-6	2.0	6.2
C_2	0.0	P_4	LJ12-6	2.3	4.7
C_2	0.0	BP_4	LJ12-6	2.3	4.7
Q_0	1.0	Q_0	LJ12-6	3.5	4.7
Q_0	1.0	Q_a	LJ12-6	4.5	4.7
Q_0	1.0	P_4	LJ12-6	5.6	4.7
Q_0	1.0	BP_4	LJ12-6	5.6	4.7
Q_a	-1.0	Q_a	LJ12-6	5.0	4.7
Q_a	-1.0	P_4	LJ12-6	5.6	4.7
Q_a	-1.0	BP_4	LJ12-6	5.6	4.7
P_4	0.0	P_4	LJ12-6	5.0	4.7
P_4	0.0	BP_4	LJ12-6	5.0	5.7
BP_4	0.0	BP_4	LJ12-6	5.0	4.7
SC_4	0.0	C_1	LJ12-6	3.1	4.7
SC_4	0.0	C_2	LJ12-6	3.1	4.7
SC_4	0.0	Q_0	LJ12-6	2.7	4.7
SC_4	0.0	P_4	LJ12-6	2.7	4.7
SC_4	0.0	BP_4	LJ12-6	2.7	4.7
SC_4	0.0	SC_4	LJ12-6	2.6	4.3

2. The validation of the CG model

For validation of the CG model, the structure compare between AA MD and CGMD, and the CMC compare between simulation and experiment were employed.

Firstly, a pre-assemble micelles composed by CTAC surfactant in the aqueous solutions were simulated by AA MD and CG MD, respectively. In the production time, the averages density profiles of micelles with respect to COM for AAMD and CGMD are displayed in Fig. S3. Consistent values show that our CG model reproduces the AA model very well. And the densities of micelle core and bulk water are close to the experimental densities of pure n-hexadecane ($0.777 g \cdot cm^{-3}$)[10] and water ($0.997 g \cdot cm^{-3}$)[11] respectively. The peak of head-groups are found to be 2.25nm,

so the surface areas per head-groups are 0.795 nm^2, this would be the equivalent of the equilibrium distance is 0.89 nm between the two head-groups of CTAC packed on the micelle, this value is almost identical to the experimental data ~0.9 nm[12].

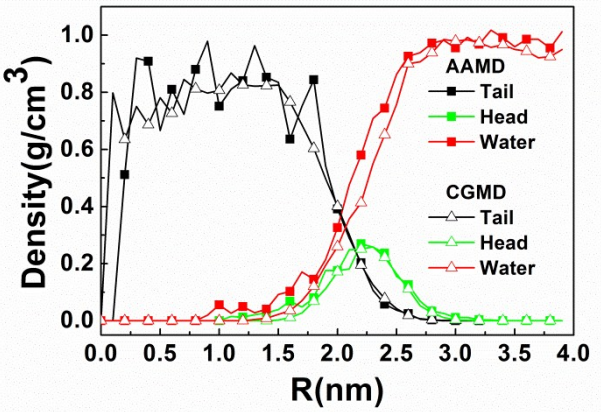

Figure S3. Density profiles of micelles with respect to COMs for AAMD (Solid-square) and CGMD (Hollow-triangle)

Further, we calculated the surfactant desorption free energy which can be used to estimate the CMC of surfactant. The calculated method for desorption free energy is same as reported by G. Larson et al.[13] , where they adopted the umbrella sampling method. Firstly, the preassembled spherical micelle consisting of 80 CTAC surfactants or 40 Gemini surfactant was constructed by Packmol[3] software and then solvated with the CG water in the box with dimensions 24×24×24 nm^3. Secondly, the energy minimization was performed on each system by the approach of steepest descent. The system was carried out in the NPT ensemble at 298 K and 1 atm for 50 ns with the time step of 0.02 ps. Periodic boundary conditions were applied in all directions. The cutoff for nonbonded interactions was set to 12 Å, where the van der Waals interaction was shifted from 0.9 to 1.2 nm and the electrostatic interaction was shifted from 0 to 1.2 nm. A fixed time step of 20 fs was used and a 100 ns simulation time was performed. The final configuration was used as the initial structure for desorption free energy simulation. In the production runs, one surfactant was selected and then pulled away from the micelle, and the center of mass (COM) of the rest

surfactant molecules was restricted in its initial position. The direction of the COM selected surfactant and the COM of the rest surfactants was select as the projection of a distance vector on an axis. The low and upper boundary were set as 3 nm and 6 nm respectively, and the wall constant was set as 10 Kcal·mol^{-1}·nm^2. The total simulation time was 200 ns. And the other settings are same as mentioned above. The change of desorption free energy escape from micelle are shown in Fig. S4. And the desorption energy ΔG is obtain by the free energy barrier, which is 12.2 kT and 25.7 kT for CTAC and 16-4-16 respectively. The CMC estimated from micelle phase separation model[14], –2kTlnCMC=ΔG, is 1.7×10^{-3} and 1.08×10^{-5}, 1.88×10^{-5} mol/L, 1.5×10^{-5} mol·L^{-1} for CTAC, 16-8-16, 16-4-16 and 16-2-16 respectively, which agree experiment in number grade[15, 16].

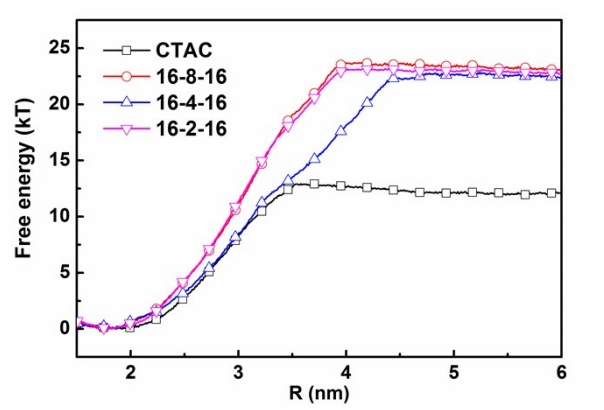

Figure S4 Free energy along the reaction coordinate for an CTAC and 16-s-16 surfactants pulled from the COM of the rest of the micelle.

In addition, the final self-assembly structures of CTAC and 16-s-16 also correspond with the observation by AAMD[5] and Cryo-TEM[12], respectively. All these results demonstrate the reliability of the CG model employed in our study.

3 Evolutions of total pairwise potential energy

The evolutions of total energy of CTAC and 16-s-16 are shown in Fig. S5, and the total pairwise potential energy for these two systems has experienced steepest

descent stage in the beginning, and then it maintains the constant. This phenomenon is also caused by the unfavorable contact between solvent and hydrophobic tails of surfactant molecule in the initial.

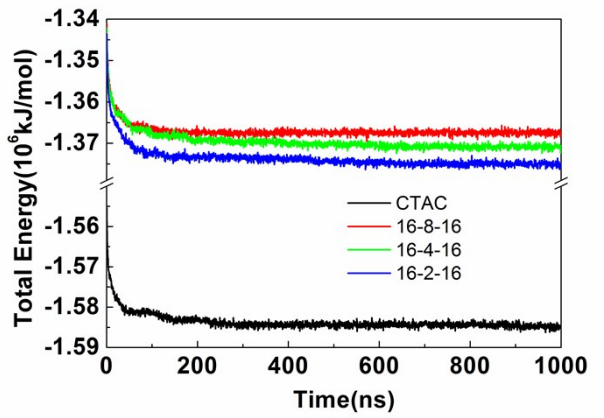

Figure S5 Evolutions of total energy for CTAC (Black line), 16-8-16 (Red line), 16-4-16 (Green line) and 16-2-16 (Blue line) aqueous solution, respectively.

4. Potential of mean force (PMF)

Two pre-assemble spherical micelles, which are constructed same as the first section (Fig. S1 (b)), are solvated with the CG water in the box with dimensions 12nm×12nm×20nm, the separation between the center of mass (COM) of the two micelles was set to 8nm. In the solutions, about 23000 CG water beads, 160 CTAC surfactants for CTAC system or 80 surfactants for 16-s-16 system were present. The modified Martini force field was used in the following simulation. The energy minimization was performed on each system by the approach of steepest descent. The two systems were carried out in the NPT ensemble at 298 K and 1 atm for 50 ns with the time step of 0.02 ps. Periodic boundary conditions were applied in all directions. In the equilibration stage, the motion of micelles was restricted to maintain their initial separation. The initial configuration for free energy calculation was shown in Fig. S6. In the production runs, equations of motions were integrated with the leapfrog algorithm with a time step of 0.02 ps. The canonical ensemble NPT was performed at 298 K and 1 atm for each system, with periodic boundary conditions along three directions. The temperature was controlled by the Berendsen thermostat[9], and the pressure coupling was set as the Berendsen barostat[9]. The cutoff for nonbonded interactions was set to 12 Å with the standard shift functions of Gromacs, where the van der Waals interaction was shifted from 0.9 to 1.2 nm and the

electrostatic interaction was shifted from 0 to 1.2 nm. A harmonic umbrella potential[13] with a force constant of 400 Kcal· mol^{-1}·nm^{-2} was applied between the COM of the two micelles using pull code. Umbrella sampling simulations were carried out in 41 different windows ranging from 8 nm to 4 nm with a sequential stepwise reduction by 0.1nm. The total simulation time for each window was 42 ns and the last 40 ns procedure was used for data analysis. The PMF was calculated from the sample windows using the Weighted Histogram Analysis Method[17] which are implemented by the *g_wham* command.

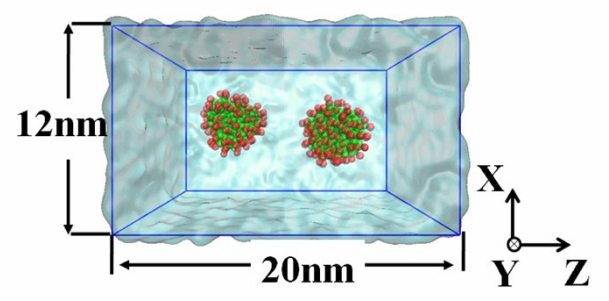

Figure S6 The initial configuration for free energy calculation

5. Solvent accessible surface area (SASA)

The effect of hydrophobic interaction is to minimize the area of contact between water and hydrophobic part of surfactant[18]. So, hydrophobic interaction can be reflected by the change of contact area. The solvent accessible surface area (SASA) between water and micelles was calculated via the 'g_sas' command embedded in Gromacs software. And the radius of the solvent probe was set as the radius of water bead.

The evolution of SASA between the hydrophobic part of surfactant and the solvent for CTAC and 16-s-16 is extracted. As shown in Fig. S7, the change of SASAs for 16-s-16 decrease regularly with the spacer length, and the variation for 16-8-16, 16-4-16, and 16-2-16 is 4.80 nm^2, 20.01 nm^2, 28.95 nm^2, respectively, which shows that the micelles composes by Gemini surfactants with shorter spacer hold the remarkable change of SASA before and after the micelles coalescence. Thus, the hydrophobic effect becomes stronger as the spacer length becomes shorter.

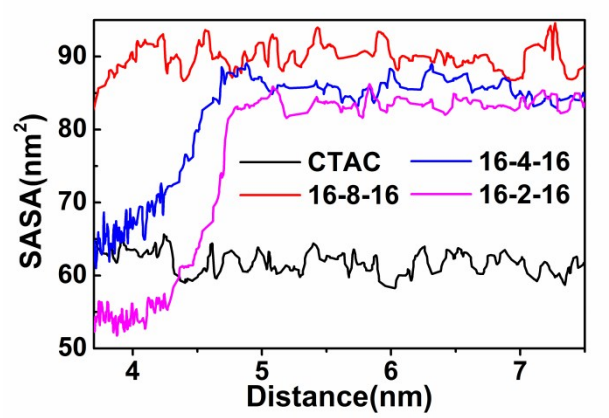

Figure S7 The change of solvent accessible surface area (SASA) between hydrophobic part of surfactant and solvent in the process of micelles coalesce for CTAC and 16-s-16.

---

6. Coarse-grain mapping, force field parameters for SDS and NaSal

The Sal^- was represented by three SC4 beads and one Q_a bead with a negative charge, and the SDS^- was represented by three C1 beads and one Q_a bead with a negative charge, these coarse-grained models has been verified and used in the study of their self-assembly[19,20]. The force field parameters are shown in Table S1 and Table S2.

References

1. S. J. Marrink, H. J. Risselada, S. Yefimov, D. P. Tieleman and A. H. de Vries, *J. Phys. Chem. B*, 2007, **111**, 7812-7824.

2. W. Shinoda, DeVane, R. and Klein, M. L, *Mol. Simul.*, 2007, **33:1**, 27-36.

3. L. Martínez, R. Andrade, E. G. Birgin and J. M. Martínez, *J. Comput. Chem.*, 2009, **30**, 2157-2164.

4. H. Berendsen, J. Grigera and T. Straatsma, *J. Phys. Chem.*, 1987, **91**, 6269-6271.

5. Z. Wang and R. G. Larson, *J. Phys. Chem. B*, 2009, **113**, 13697-13710.

6. S. Pal, B. Bagchi and S. Balasubramanian, *J. Phys. Chem. B*, 2005, **109**, 12879-12890.

7. M. Jorge, *Langmuir*, 2008, **24**, 5714-5725.

8. B. Hess, C. Kutzner, D. van der Spoel and E. Lindahl, *J. Chem. Theory Comput.*, 2008, **4**, 435-447.

9. H. J. C. Berendsen, J. P. M. Postma, W. F. van Gunsteren, A. DiNola and J. R. Haak, *J. Chem. Phys.*, 1984, **81**, 3684.

10. W. M. Haynes, Handbook of Chemistry and Physics, CRC Press, 93rd edn, 2012.
11. C. L.Yaws, Chemical Properties Handbook. McGraw-Hill, New York, 1999
12. D. Danino, Y. Talmon and R. Zana, *Langmuir*, 1995, **11**, 1448-1456.
13. A. Leach, *Molecular Modelling: Principles and Applications* Prentice Hall, 2 edn., 2001.
14. F. M. Menger and C. E. Portnoy, *J. Am. Chem. Soc.*, 1967, **89**, 4698-4703.
15. E. Roelants, E. Geladé, J. Smid and F. De Schryver, *J. Colloid Interface Sci.*, 1985, **107**, 337-344.
16. R. Zana, *Adv. Colloid Interface Sci.*, 2002, **97**, 205-253.
17. S. Kumar, J. M. Rosenberg, D. Bouzida, R. H. Swendsen and P. A. Kollman, *J. Comput. Chem.*, 1992, **13**, 1011-1021.
18. D. Chandler, *Nature*, 2005, **437**, 640-647.
19. S. Jalili and M. Akhavan, *Colloids Surf., A*, 2009, **352**, 99-102.
20. A. V. Sangwai and R. Sureshkumar, *Langmuir*, 2011, **27**, 6628-6638.